JOURNAL OF GEOPHYSICAL RESEARCH, VOL. 92, NO. D6, PAGES 6614–6626, JUNE 20, 1987

Atmospheric Distribution of ^{85}Kr Simulated With a General Circulation Model

DANIEL J. JACOB

Center for Earth and Planetary Physics, Harvard University, Cambridge, Massachusetts

MICHAEL J. PRATHER

NASA Goddard Space Flight Center Institute for Space Studies, New York

STEVEN C. WOFSY AND MICHAEL B. MCELROY

Center for Earth and Planetary Physics, Harvard University, Cambridge, Massachusetts

A three-dimensional chemical tracer model for the troposphere is used to simulate the global distribution of ^{85}Kr, a long-lived radioisotope released at northern mid-latitudes by nuclear industry. Simulated distributions for the period 1980–1983 are in excellent agreement with data from six latitudinal profiles measured over the Atlantic. High concentrations of ^{85}Kr are predicted over the Arctic in winter, advected from European sources, and somewhat smaller enhancements arising from the same sources are predicted over the tropical Atlantic in summer. Latitudinal gradients are steepest in the northern tropics, with distinctly different seasonal variations over the Pacific, as compared to the Atlantic. The global inventory of ^{85}Kr is reconstructed for the period 1980–1983 by combining the concentrations measured over the Atlantic with the global distributions predicted by the model. The magnitude of the Soviet source is derived. The interhemispheric exchange time is calculated as 1.1 years, with little seasonal dependence.

1. INTRODUCTION

This paper describes an attempt to simulate the spatial distribution of atmospheric ^{85}Kr, a radioisotope (half-life 10.76 years) emitted during reprocessing of nuclear fuel. There are only a few known sources of ^{85}Kr, all in the northern hemisphere and all confined to a narrow band of latitudes between 33° and 53°N. Release of ^{85}Kr is directly related to production of plutonium [*Schroder and Roether*, 1975]. Emissions from western sources, mainly in the United Kingdom, France, and the United States, are well documented. There has been considerable interest in using atmospheric measurements of ^{85}Kr to monitor Soviet production of plutonium [*Von Hippel et al.*, 1985]. However, measurements are necessarily limited in space and time. To derive global quantities, they must be placed in a larger context. A three-dimensional model incorporating relevant features of the atmospheric circulation provides this facility. We report results of such an analysis here, using a chemical tracer model (CTM). Winds, temperature, and convection statistics used in the CTM are obtained from a general circulation model of the atmosphere (GCM) developed by the Goddard Institute for Space Studies [*Hansen et al.*, 1983].

Our long-range objective in developing the CTM is to describe the global distributions of tropospheric O_3, CO, NO_x, and other trace species. The model in this case must account properly for exchange with the stratosphere, for a range of chemical processes in the troposphere, and for reactions at the surface. It must simulate correctly the redistribution of chemicals spatially within the atmosphere, including exchange between hemispheres. We have elected to approach this objective through a series of intermediate steps. Our first study involved the long-lived chlorofluorocarbons CFC-11 and CFC-12 [*Prather et al.*, this issue]. The production and release history of these gases are relatively well known. Concentrations have been monitored extensively at a few sites over the world during the last decade. Loss of CFCs is due mainly to photolysis in the stratosphere. Simulation of the global distribution and comparison with observations provides an excellent check on the ability of the model to describe long-range transport of chemicals. We found that the model gave an excellent representation of the distribution of CFCs within the individual hemispheres. Simulation of interhemispheric transport was less successful. We concluded that transport on scales below the resolution of the GCM could be important in this context. This transport was treated as a diffusive process associated with deep convection, and a length scale was selected to fit the observations. The present study of ^{85}Kr provides an independent check on this parameterization. It offers an additional important opportunity to test the capability of the model to treat intrahemispheric transport, in that the source of ^{85}Kr is spatially more confined than that of CFCs and in that the spatial distribution of ^{85}Kr has been defined observationally by several detailed latitudinal profiles, data lacking for CFCs. As we shall see, the model is successful not only for CFCs but also for ^{85}Kr, lending confidence to the validity of the overall approach.

Von Hippel et al. [1986] discussed the increase in the global inventory of ^{85}Kr since 1945, using data primarily from north-south oceanic cruises conducted in 1964, 1972, and 1983 [*Pannetier*, 1970; *Karol' et al.*, 1976; W. Weiss, unpublished data, 1986]. They calculated global inventories from the measured latitudinal profiles, assuming that ^{85}Kr was longitudinally and vertically well-mixed within the troposphere. The strato-

Paper number 7D0362.
0148-0227/87/007D-0362$05.00

spheric burden was taken to constitute a fixed fraction of the tropospheric burden, with scaling coefficients adopted from *Telegadas and Ferber* [1975]. Von Hippel et al. inferred a continued growth of Soviet emissions between 1972 and 1983 and concluded that the Soviet Union had not cut back its production of plutonium during that period.

Six data sets defining latitudinal concentration profiles for ^{85}Kr were collected on cruises in the Atlantic between 1980 and 1983 (*Weiss et al.* [1983]; also, data from W. Weiss reported by *Von Hippel et al.* [1986]). From these, one may attempt to reconstruct the recent trend in the global inventory of ^{85}Kr. The increase in ^{85}Kr abundances during this period is small, however, relative to the preexisting inventory. Consequently, care must be exercised to minimize uncertainties in analyses of spatially limited surface measurements. The assumptions concerning the global distributions of ^{85}Kr used by *Von Hippel et al.* [1986] should be acceptable when large differences in inventory are involved (such as between 1972 and 1983) but may be inadequate for resolving changes on shorter time scales because of neglect of details in the general circulation. A more accurate scaling of Atlantic surface data to the global atmosphere can be derived using global distributions of ^{85}Kr from a three-dimensional model.

Several investigators have previously employed latitudinal profiles of ^{85}Kr concentrations to examine the meridional circulation. *Pannetier* [1970] used data from a 1964 Atlantic cruise to derive characteristic times for exchange of air between mid-latitudes and the tropics. *Telegadas and Ferber* [1975] proposed a schematic representation of the stratospheric circulation based on a set of measurements from 1973. *Karol' et al.* [1976] fitted the data of *Pannetier* [1970], *Telegadas and Ferber* [1975], and results from a 1972 Soviet cruise to a two-dimensional circulation model, assuming an exponentially growing global source. In addition, *Weiss et al.* [1983] used data from their Atlantic cruises to estimate meridional diffusion coefficients and rates of interhemispheric exchange.

We will compare here the latitudinal gradients over the Atlantic observed in 1980–1983 to those simulated by the CTM. The spatial distribution of ^{85}Kr derived from the CTM will be used in conjunction with the available cruise data to define the recent trend in the ^{85}Kr global inventory. The global distribution of ^{85}Kr in the troposphere and its seasonal dependence will be discussed. The utility of surface measurements for determining features of the meridional circulation will be evaluated.

2. Model Description

The spatial distribution of ^{85}Kr was obtained by solving the appropriate three-dimensional continuity equation, using the model described by *Prather et al.* [this issue]. The CTM was run with dynamical variables from a GCM developed at the Goddard Institute for Space Studies [*Hansen et al.*, 1983]. The GCM has a horizontal resolution of 4° latitude × 5° longitude, with nine layers in the vertical. The layers are distributed from the surface to 10 mbar and are prescribed following σ coordinates, as described by *Phillips* [1957], *Hansen et al.* [1983], and *Prather et al.* [this issue]. There are seven layers in the troposphere, extending from the surface to about 150 mbar; the upper atmosphere is represented by two layers, 150–70 mbar and 70–10 mbar. The GCM was initialized with climatological data for January 1, and was run for a model time of 27 months. Wind fields, surface pressures, and convection statistics from the last 12 months of the run (April 1 to March 31) were saved as input to the CTM. Mean horizontal winds and surface pressures were saved every 4 hours, and mean frequencies for convective exchange between pairs of vertical layers were saved every 5 days. The CTM uses an 8° × 10° grid with a time step of 8 hours. The meteorological input to the CTM was obtained by averaging the GCM output over four contiguous 4° × 5° boxes. The same GCM model year was used for all CTM simulations.

Transport of ^{85}Kr in the CTM proceeds by advection, convection, and diffusion. Advection of tracer is calculated from the tracer concentration field and the GCM winds, using an upstream method conserving mass and first-order moments of tracer concentration [*Russell and Lerner*, 1981]. Vertical wind velocities are calculated from the horizontal convergence and the change in surface pressure. The treatment of convective transport is discussed in detail by *Prather et al.* [this issue]. Convection frequencies from the 5-day average convection statistics are used to determine the fraction of air within a grid box that is transported vertically by convection at each time step. When a column of air is unstable with respect to a dry adiabat, the air is assumed to mix uniformly within the column. When a column of air is unstable with respect to a moist adiabat, 50% of the air in the lowest layer is moved directly to the highest layer that can be attained given the available moist static energy, with no entrainment, followed immediately by subsidence over all vertical layers in the column. Horizontal motions due to convection generally proceed over length scales smaller than the 4° × 5° GCM grid box and are therefore ignored in the model calculations. It is recognized, however, that deep convective vertical motions may be associated with large convective complexes, which can result in significant horizontal redistribution of tracer between adjacent grid boxes. This horizontal transport is modeled as a diffusive process, with a length scale D, and is computed according to the frequency of deep convection calculated by the GCM (see *Prather et al.* [this issue] for the formulation of the convective diffusion coefficient). We found that a length scale $D = 180$ km provides an excellent fit to the ^{85}Kr cruise data, and we selected this value for all simulations. A length scale of this magnitude is consistent with observed sizes of large convective complexes in the tropics [*Houze and Hobbs*, 1982], and with the results of the CFC study by *Prather et al.* [this issue].

Emissons of ^{85}Kr from non-Soviet sources (Table 1 and Figure 1) were taken from *Von Hippel et al.* [1986]. Emissions were prorated over the year and added at each time step to the lowest layer of the troposphere in the appropriate grid box. Exchange with the oceans was neglected because of the low solubility of Kr. No flux was allowed through the upper boundary of the top layer at 10 mbar. The only sink for atmospheric ^{85}Kr was assumed to be radioactive decay, with an e-folding lifetime $\tau_d = 15.52$ years.

We assumed that the Soviet release was concentrated near Kyshtym (55°N, 60°E), a major site for nuclear fuel reprocessing (F. Von Hippel, Princeton University, private communication, 1986). In reality, the Soviet source is probably distributed over several major release sites. The uncertainty in location of the Soviet source should have little effect on predicted meridional transport, since the release sites are most likely located in the same latitudinal band of the CTM as

TABLE 1. Emissions of ^{85}Kr

	1978	1979	1980	1981	1982	1983
Savannah River, U.S.A. (33°N, 81°W)	0.48	0.46	0.47	0.54	0.56	0.69
Idaho City, U.S.A. (44°N, 116°W)	0.10	0.00	0.09	0.06	0.01	0.00
Sellafield, U.K. (53°N, 3°W)	0.70	0.94	0.84	1.40	1.19	1.13
Marcoule, France (44°N, 4°E)	0.31	0.28	0.54	0.31	0.31	0.31
La Hague, France (50°N, 2°W)	0.79	0.64	0.83	0.91	1.27	1.95
Karlsruhe, F.R.G. (49°N, 8°E)	0.00	0.05	0.03	0.00	0.00	0.08
Tokai-Mura, Japan (35°N, 140°E)	0.06	0.00	0.28	0.11	0.19	0.09
Soviet Union						
preliminary estimate	3.41	3.62	3.03	2.91	2.84	2.24
revised estimate	3.56	3.77	3.19	3.07	3.00	2.40
Global	6.00	6.13	6.27	6.40	6.53	6.66

Emissions are stated in megacuries per year and are totaled over the calendar year. Non-Soviet emissions are taken from *Von Hippel et al.* [1986]. Global emissions are computed using equation (4) and include the revised estimate of the Soviet source.

Kyshtym (48°–56°N) or in the adjacent band to the north (56°–64°N). Surface concentrations predicted over the Atlantic should not be affected by details of the Soviet plume, which would be advected usually to the east and north.

Concentrations of ^{85}Kr are given in units of picocuries per cubic meter of air at standard temperature and pressure, abbreviated here as pCi/SCM (i.e, pCi/m^3 STP). A concentration of 1 pCi/SCM is equivalent to a mixing ratio of ^{85}Kr of 6.82×10^{-19} vol/vol. Inventories and emissions are given in units of megacuries (MCi); one megacurie is equivalent to 2.55 kg of ^{85}Kr. The total mass of the atmosphere is 5.06×10^{18} kg, so that the global inventory of ^{85}Kr, I (in megacuries) can be obtained by multiplying the global mean atmospheric concentration $\langle C \rangle$ (in pCi/SCM) by 3.92.

3. Model Results

3.1. *Determination of the Soviet Source*

The magnitude of the Soviet source was determined by subtracing the well-defined non-Soviet sources from the global emission rate estimated on the basis of model simulations. A preliminary estimate of the global emission rate was derived from the Atlantic cruise data, using the approach of *Von Hippel et al.* [1986]. The cruise data were interpolated to give average concentrations for each of the 8° × 10° CTM latitudinal bands (Table 2). Concentrations reported at the most northerly latitudes (44°–54°N, depending on the cruise) were extrapolated to higher latitudes in the northern hemisphere; a similar assumption was used for concentrations at high latitudes in the south. We calculated in this manner a mean surface concentration $\langle A \rangle$ at 30°W longitude (middle of the Atlantic), by using an appropriate areal weighting of concentrations measured in each latitudinal band. A preliminary estimate of the global mean atmospheric concentration, $\langle C_p \rangle$, was then calculated from $\langle A \rangle$ by assuming that ^{85}Kr was well-mixed longitudinally and vertically to 150 mbar (through layer 7). The concentrations of ^{85}Kr in the eighth (150–70 mbar) and ninth layers (70–10 mbar) were taken as 87 and 54%, respectively, of the concentrations in the lowest layers, on the basis of the stratospheric data of *Telegadas and Ferber* [1975]. With this correction for the fraction of the inventory in the stratosphere, $\langle A \rangle$ was related to $\langle C_p \rangle$, using a coefficient $R_p = \langle C_p \rangle / \langle A \rangle = 0.957$.

Values of $\langle C_p \rangle$ calculated in this manner for the six 1980–1983 cruises can be fitted with a linear regression to provide a

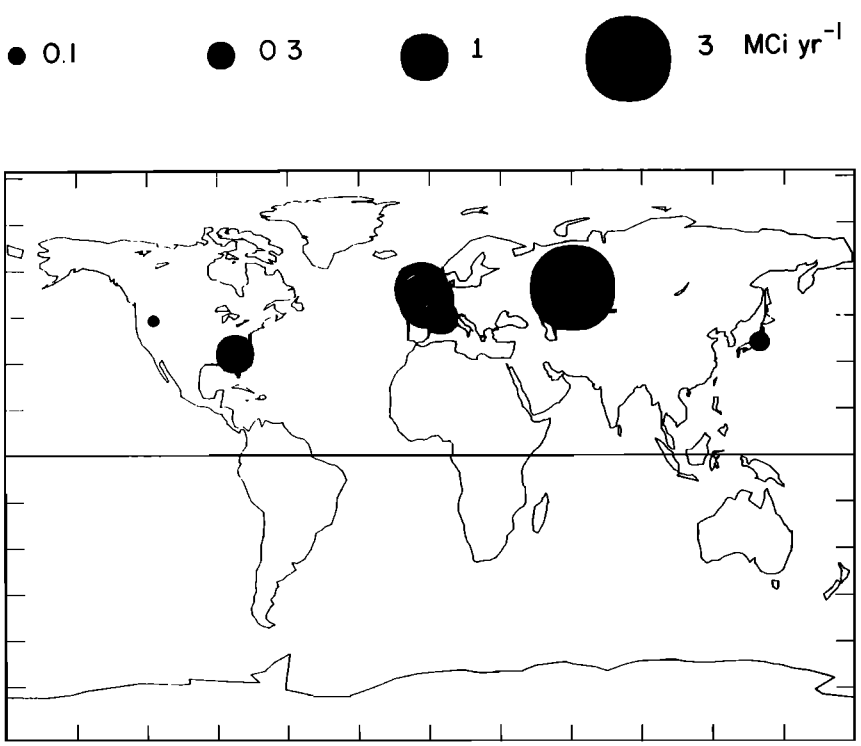

Fig. 1. Major sources of ^{85}Kr and average emission rates for 1980–1983.

TABLE 2. Concentrations of ^{85}Kr Measured on Atlantic Cruises and Calculated Global Mean Concentrations

	Oct. 1980	April 1981	Jan. 1982	Feb. 1983	March 1983	Oct. 1983
52°N	18.9	20.1	20.3	20.4	20	22.0
44°N	18.6	20.0	19.3	20.4	20.9	20.0
36°N	18.4	19.1	19.3	19.1	20.3	19.8
28°N	18.4	19.4	19.2	19.5	20.0	20.1
20°N	17.8	19.1	19.2	19.8	19.5	19.8
12°N	16.7	18.8	19.0	19.5	19.4	18.4
4°N	16.4	16.9	18.0	19.2	18.6	18.0
4°S	16.4	16.6	17.3	17.6	17.9	17.5
12°S	16.5	16.5	16.7	17.4	17.8	17.4
20°S	16.0	16.4	16.9	17.5	17.3	17.5
28°S	15.9	16.2	17.0	17.3	17.3	
36°S		16.4	16.6	17.0	17.3	
44°S			16.7	16.9	17.4	
52°S			16.5	17.0	17.2	
60°S			16.4	17.0	17.0	
68°S			16.5	17.0	17.5	
76°S				16.9	17.3	
84°S				16.8	17.2	
$\langle A \rangle$	17.0	17.8	18.0	18.5	18.7	18.7
R	0.989	0.980	0.988	0.982	0.976	0.989
$\langle C \rangle$	16.8	17.4	17.8	18.2	18.3	18.5
ΔA (observed)	1.9 ± 0.3	2.7 ± 0.3	2.5 ± 0.3	2.5 ± 0.3	2.5 ± 0.3	2.5 ± 0.3
ΔA (model)	2.2	2.8	2.5	2.8	2.9	2.5
ΔC (model)	1.7	1.7	1.8	1.7	1.7	1.9

Concentrations are stated in pCi/SCM. Measured latitudinal profiles from W. Weiss and colleagues [*Weiss et al.*, 1983; *Von Hippel et al.*, 1986], interpolated over the 8° × 10° CTM grid. Standard errors on the measurements are about 1% [*Weiss et al.*, 1983]. $\langle A \rangle$ is the mean surface concentration at 30°W longitude, calculated by weighting the cruise data in each latitudinal band by the area of the equivalent zonal band. Data from the northernmost and southernmost latitudes of the cruises are extrapolated to the higher latitudes. R is a model-derived coefficient scaling $\langle A \rangle$ to $\langle C \rangle$ (see text). $\langle C \rangle = R\langle A \rangle$ is the global mean atmospheric concentration. $\Delta A = \langle A_N \rangle - \langle A_S \rangle$ is the difference in hemispheric mean surface concentrations at 30°W longitude. $\Delta C = \langle C_N \rangle - \langle C_S \rangle$ is the difference in global hemispheric mean concentrations.

preliminary estimate for the global inventory I_p (in megacuries):

$$I_p = 62.8 + 2.0(T - 1980.0) \quad (1)$$

where T is years (A.D.). The corresponding global emission rate E_p (in megacuries per year) is

$$E_p = 6.05 + 0.13(T - 1980.0) \quad (2)$$

from which a preliminary estimate of the Soviet source may be derived (Table 1). We conducted a preliminary 4-year model run (1978–1981) with this estimated source function. The initial distribution for January 1, 1978 (1978.0) was prescribed, using the latitudinal profile measured in October 1980, scaled by a factor of 0.913 to account for the difference in global inventory between 1978.0 and October 1983 (1983.8) (equation (1)). The tracer was initially well-mixed longitudinally and vertically through the seventh layer. Initial concentrations for the eighth and ninth layers were set with the scaling factors given above.

The interhemispheric differences and latitudinal gradients predicted in this run were found to give reasonably good agreement with the 1980–1981 Atlantic measurements. This agreement indicates that the CTM simulates realistically the meridional transport of ^{85}Kr, considering that the latitude of the adjustable Soviet source is relatively well defined. However, the simulated concentrations over the surface of the Atlantic were systematically lower than observed at all latitudes. We concluded that the global emission rate given by (2) is too low. Since the CTM appears to provide a reasonable picture of ^{85}Kr transport, the global distributions obtained from the preliminary run may be used to derive an improved estimate of the global emission rate. New scaling coefficients, $R = \langle C_p \rangle / \langle A_p \rangle$, were calculated from the model simulation for each month, on the basis of the mean surface concentration at 30°W longitude, $\langle A_p \rangle$. These coefficients were used in conjunction with the value $\langle A \rangle$, determined from the cruise data, to obtain an improved estimate of the global mean atmospheric concentration, $\langle C \rangle = R\langle A \rangle$ (Table 2). Values of R range from 0.976 to 0.989, significantly greater than R_p. A linear fit to $\langle C \rangle$ versus time (Figure 2) gives the following expression for the global inventory I (in megacuries):

$$I = 65.2 + 2.0(T - 1980.0) \quad (3)$$

The corresponding global emission rate E (in megacuries per year) is

$$E = 6.20 + 0.13(T - 1980.0) \quad (4)$$

An improved estimate of the Soviet source can be calculated from (4), and is shown in Table 1. The Soviet source is about 5% larger than the preliminary estimate; a 25% decline is noted between 1980 and 1983.

The above procedure for deriving the global emission rate was iterated. A 6 year simulation (1978–1983) was conducted, using the revised estimate of the Soviet source, and new scaling coefficients were computed on the basis of this simulation. Global inventories calculated from these scaling coefficients

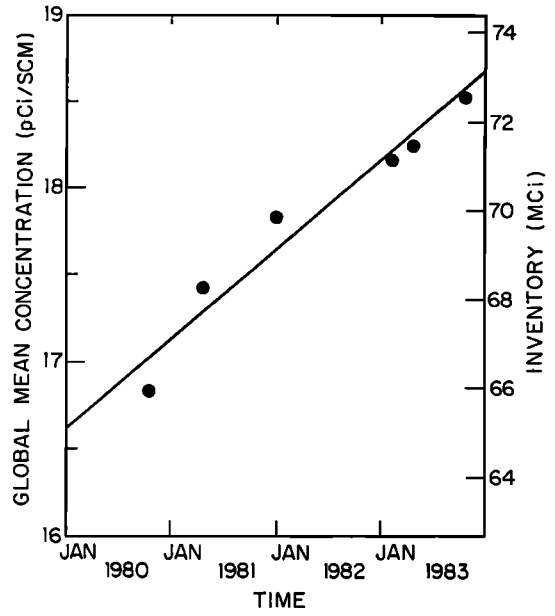

Fig. 2. Global inventory of ^{85}Kr derived from the model simulations. The line is a linear regression to the six points.

were 0.1% lower than those given by (3); the temporal trend was identical. Therefore the procedure converges rapidly, and the global source as given by (4) is sufficiently accurate for our purposes. The 1978–1983 simulation was used to evaluate the model performance against the Atlantic cruise data and to examine further the global atmospheric distribution of ^{85}Kr. Results are discussed in the following sections.

It is worth noting that the preliminary calculation based on the simple assumptions of *Von Hippel et al.* [1986] gave a surprisingly accurate estimate of the global inventory. One main reason for this result is that the Atlantic is usually very far downwind of the European and Soviet plumes, thus vertical gradients of ^{85}Kr above the Atlantic are fairly small. Further, the overestimate caused by generalizing Atlantic surface concentrations to the air column up to 150 mbar is compensated by underestimates due to (1) the lack of measurements in the Arctic where the model predicts high concentrations, and (2) the delay in transport from source regions to the Atlantic.

Simulated yearly mean concentrations of ^{85}Kr in the 150–70 mbar and 70–10 mbar layers are 95 and 89% of the tropospheric mean, respectively, for the 1980–1983 model years. The stratospheric contribution to the global inventory is predicted to be larger than that determined by *Telegadas and Ferber* [1975]. The Telegadas and Ferber data were collected in 1973, at a time when the ^{85}Kr concentration was increasing rapidly [*National Council on Radiation Protection and Measurements*, 1975]. Since then, the rate of increase has declined considerably [*Grossman and Holloway*, 1985]. As a result, the stratosphere is expected to contain a larger fraction of the global ^{85}Kr inventory at present than in 1973.

3.2. *Comparison With Observations*

Surface concentrations predicted at 30°W (middle of the Atlantic) and 10°W (eastern edge of the Atlantic) are compared to the cruise data in Figure 3. Remarkably good agreement is shown between model predictions and measurements for all cruises, indicating that the CTM provides a good simulation of meridional transport. A sensitive measure of the CTM performance is given by a comparison of the predicted and observed interhemispheric differences in the surface concentrations over the Atlantic, $\Delta A = \langle A_N \rangle - \langle A_S \rangle$, where $\langle A_N \rangle$ and $\langle A_S \rangle$ define hemispheric mean surface concentrations along the longitude of the cruise tracks. The interhemispheric differences calculated from the measurements are compared with the model results in Table 2. Agreement is excellent.

Proper simulation of the latitudinal profiles is dependent, in part, on the value adopted for D. *Prather et al.* [this issue] have discussed the sensitivity of model predictions to D in the case of CFCs. They concluded that values of D in the range 180–250 km were appropriate for simulating the concentrations and trends observed for CFCs at fixed sites. The lower end of the range provided generally the better results. We find in the present study that $D = 180$ km provides a better simulation of the meridional transport of ^{85}Kr than $D = 250$ km. We show in Figure 4 simulations of the 1980–1982 Atlantic cruise data, using either value of D. The model run with $D = 250$ km produces excessive smoothing of the latitudinal gradients and insufficient interhemispheric concentration differences. From the point of view of model evaluation, it is encouraging that $D = 180$ km provides an excellent simulation of observations for both ^{85}Kr and CFCs. An important result of the ^{85}Kr study is that both the overall interhemispheric differences and the latitudinal gradients in concentrations are reproduced correctly, over a variety of seasons.

The predicted surface concentrations of ^{85}Kr at 10° and 30°W are similar south of 40°N, but they are notably different at northern mid-latitudes and in the Arctic (Figure 3). The higher concentrations at 10°W are due to westward advection from European sources. The model predicts peak concentrations at about 60°N; unfortunately, measurements at high latitudes in the northern hemisphere are currently lacking.

Most of the ^{85}Kr data available, aside from the Atlantic cruises, are from sites in Europe influenced directly by local sources [*Weiss et al.*, 1983]. These data cannot properly be analyzed with an 8° × 10° CTM grid, or even a 4° × 5° grid, since plumes of ^{85}Kr-enriched air are expected to be present on scales smaller than a grid box. Available data for the rest of the world are scarce. A 1972–1983 record of ^{85}Kr from a 500 × 500 km network of 27 stations in and around the Nevada Weapons Test Site has been reported [*Grossman and Holloway*, 1985]. On-site stations had values only slightly higher than off-site stations (by about 0.6 pCi/SCM). Concentrations did not significantly decrease with increasing distance from the test site, so that leakage from underground tests would not appear to provide an important local source.

Concentrations reported for Nevada by *Grossman and Holloway* [1985] increased approximately linearly between 1980 and 1983, from 21.0 pCi/SCM in 1980 to 24.8 pCi/SCM in 1983. By way of comparison, concentrations predicted by the model for Nevada increased from 18.5 pCi/SCM in 1980 to 20.0 pCi/SCM in 1983. Both the concentrations and the relative rate of increase predicted by the model are substantially lower than observed. This discrepancy may reflect problems with calibration of the measurement techniques. The concentrations measured by *Grossman and Holloway* [1985] are systematically higher by 2–5 pCi/SCM than concentrations measured in West Germany and Belgium by independent investigators over the same period [*Von Hippel et al.*, 1986]. This difference is inconsistent with the geographical distribution of sources (Figure 1).

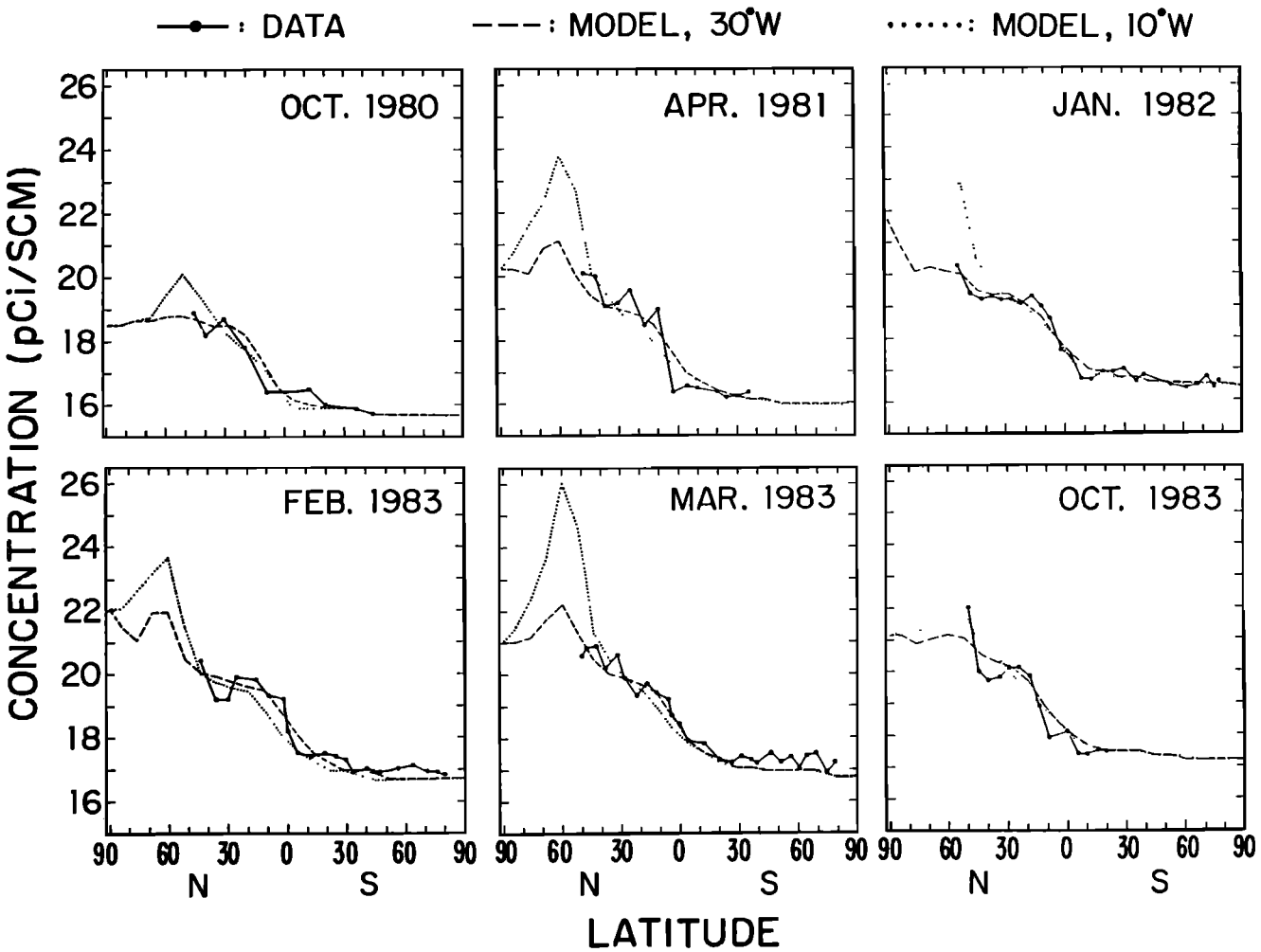

Fig. 3. Latitudinal profiles of ^{85}Kr surface concentrations over the Atlantic, measured by W. Weiss (solid line) and predicted by the model at 30°W (dashed line) and at 10°W (dotted line).

3.3. *Global Distribution of ^{85}Kr*

Global distributions of ^{85}Kr are shown in Figures 5–8 for 4 months in 1983: January, April, July, and October. We present the following features: (1) maps of surface concentrations, (2) cross sections of concentration as a function of latitude and altitude at 30°W, (3) longitudinal cross sections at 44°N, (4) similar results for 60°N. Differences between the months primarily reflect the seasonality of transport but also reflect a small temporal increase in the global inventory (0.4 pCi/SCM between January and October). The distribution in the southern hemisphere is remarkably homogeneous. On the other hand, large seasonal differences are noted in the north. Important longitudinal and vertical gradients are apparent in the lower troposphere at northern mid-latitudes, in particular the presence of two distinct plumes over the Soviet Union and western Europe. Smaller plumes from the United States and Japan are evident in the cross sections at 44°N but are undetectable at 60°N.

In January (Figure 5) the ^{85}Kr plumes are trapped in the lower layers of the atmosphere as a result of the lack of convective activity. The plumes are advected eastward and poleward within the lower troposphere, providing high concentrations at the surface over all of Europe, the Soviet Union, and the Arctic. Steep vertical gradients are predicted in plume regions from the ground to about 700 mbar, with much weaker gradients at higher altitudes. The plumes are undetectable above 600 mbar in the cross sections at 44° and 60°N.

In July (Figure 7), convection over the Eurasian continent efficiently transports ^{85}Kr upward to the middle and high troposphere. Mean concentrations at the surface are lower than in January. The general circulation is weaker in summer, and eastward transport in the lower layers is less extensive. As a result, surface concentrations over the Arctic and the eastern Soviet Union in July show no detectable impact from the European and Soviet plumes. Some direct transport of ^{85}Kr from western Europe to the tropical Atlantic is predicted in the lower troposphere and appears in the 30°W cross section as a low-altitude layer of high concentration extending south to 15°N. Most of the eastward transport of ^{85}Kr plumes takes place in the middle troposphere, resulting in a layer of high concentration between 550 and 250 mbar over Asia and the northern Pacific.

The seasonal trend of pollutant transport from Europe to the Arctic, as simulated by the model for ^{85}Kr, is consistent with recent measurements of atmospheric composition at Arctic sites [*Rahn*, 1985]. In particular, concentrations of secondary aerosol in Alaska and northern Canada are found to be considerably higher in winter than in summer [*Rahn and McCaffrey*, 1980; *Barrie and Hoff*, 1985]. The high wintertime

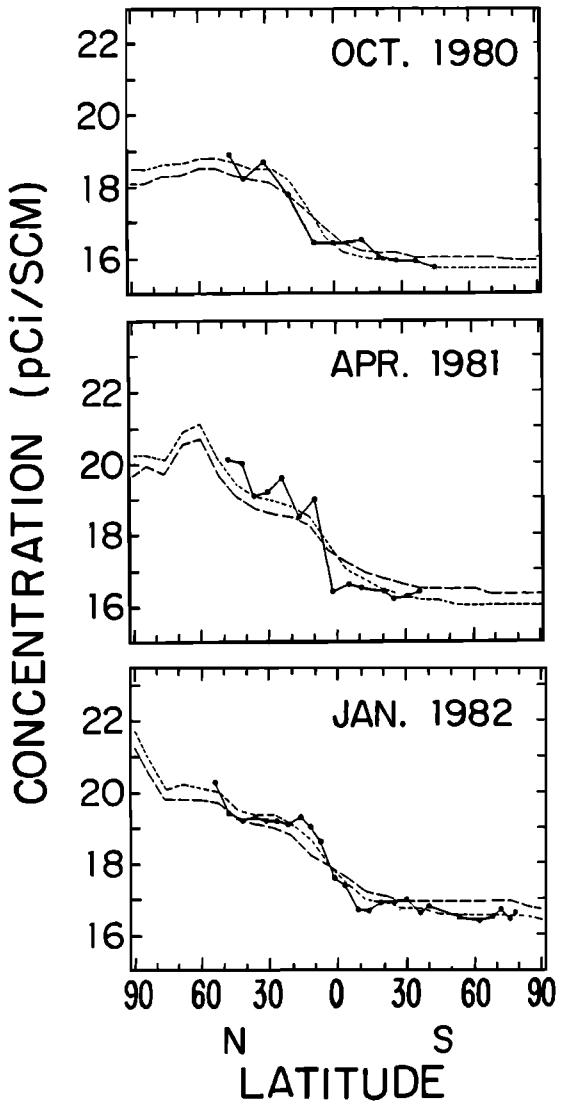

Fig. 4. Latitudinal profiles of ^{85}Kr surface concentrations over the Atlantic, measured by W. Weiss (solid line) and predicted at 30°W by the model run with D = 180 km (short dashes) and with D = 250 km (long dashes).

concentrations are attributed to transport from the Soviet Union and from Europe [*Lowenthal and Rahn*, 1985]. *Barrie and Hoff* [1985] observe that pollution in the Arctic is usually confined to the lower troposphere, a result consistent with our model predictions.

The surface distribution of ^{85}Kr shows less longitudinal structure in the northern tropics than at mid-latitudes. Southward intrusions of ^{85}Kr plumes are infrequent. An exception is the influence of European sources on the tropical Atlantic in summer. The main feature of the ^{85}Kr distribution in the northern tropics is a steep latitudinal gradient maintained between high concentrations at northern mid-latitudes and low concentrations south of the equator. From the structure of this gradient, it appears that most of the resistance to global meridional transport of ^{85}Kr takes place in the northern tropics. Similar gradients have been reported for other tracers with dominant sources in the northern hemisphere, such as CH_4 [*Heidt et al.*, 1980; *Khalil and Rasmussen*, 1983; *Steele et al.*, 1987].

The latitudinal gradients of ^{85}Kr concentration over the surface of the Atlantic vary significantly between January and July. In January, concentrations increase steadily from the equator to the Arctic. In July the gradient is confined to a narrow latitudinal band from the equator to 15°N and is much steeper. These seasonal differences in the latitudinal profiles over the Atlantic are due not to changes in the global rate of meridional transport, but rather to variations in low-altitude longitudinal advection from sources at northern mid-latitudes. Latitudinal profiles at other longitudes are predicted to show different seasonal behavior, as indicated by the surface maps in Figures 5–8. Pacific cruises, in particular, should show steeper latitudinal gradients in winter than in summer, as a consequence of more efficient wintertime advection of the Soviet plume in the lower troposphere over the North Pacific. It would be easy therefore to draw erroneous conclusions concerning global budgets and trends on the basis of isolated surface measurements. Interpretation of such data in the context of a three-dimensional model has obvious advantages.

Concentrations of ^{85}Kr observed over West Germany [*Weiss et al.*, 1983] show a strong seasonality with peak values in the winter and minimum values in summer. This pattern is consistent with model predictions and is attributed to increased ventilation of the boundary layer in summer due to enhanced convective activity. Seasonal variability in the Nevada data, on the other hand, is insignificant [*Grossman and Holloway*, 1985]. Nevada is far from sources and should be relatively unaffected by seasonal variations in transport.

3.4. *Interhemispheric Exchange*

The homogeneity of ^{85}Kr concentrations in the southern hemisphere indicates that the time scale for interhemispheric exchange is longer than that for mixing within a hemisphere. We may define an interhemispheric exchange time for ^{85}Kr, τ_{ex}, as the residence time for excess ^{85}Kr in the northern hemisphere:

$$\tau_{ex} = \frac{\Delta C}{\phi_{N\to S}} \tag{5}$$

where $\Delta C = \langle C_N \rangle - \langle C_S \rangle$, $\langle C_N \rangle$ and $\langle C_S \rangle$ are global mean hemispheric concentrations, and $\phi_{N\to S}$ is the net cross-equatorial flux. We calculate a mean value for τ_{ex} of 1.1 years for each of the model years, using annual means of the individual quantities in (5). A similar value of τ_{ex} was reported for CFCs by *Prather et al.* [this issue].

In an idealized two-box model the interhemispheric difference ΔC evolves with time according to

$$\frac{d\Delta C}{dt} = \frac{E}{1.96} - (2\tau_{ex}^{-1} + \tau_d^{-1})\Delta C \tag{6}$$

If the relative rate of increase in the inventory is small compared to the rate of interhemispheric exchange, ΔC should approach a steady state value. This condition is satisfied for the period 1980–1983, during which the ^{85}Kr inventory increased at a rate of only about 3% per year. Indeed, the interhemispheric differences calculated from the Atlantic cruise data remained relatively constant between 1980 and 1983 (Table 2). The interhemispheric exchange time can then be computed from the steady state value of ΔC:

$$\tau_{ex} = \left(\frac{E}{3.92\Delta C} - \frac{1}{2\tau_d}\right)^{-1} \tag{7}$$

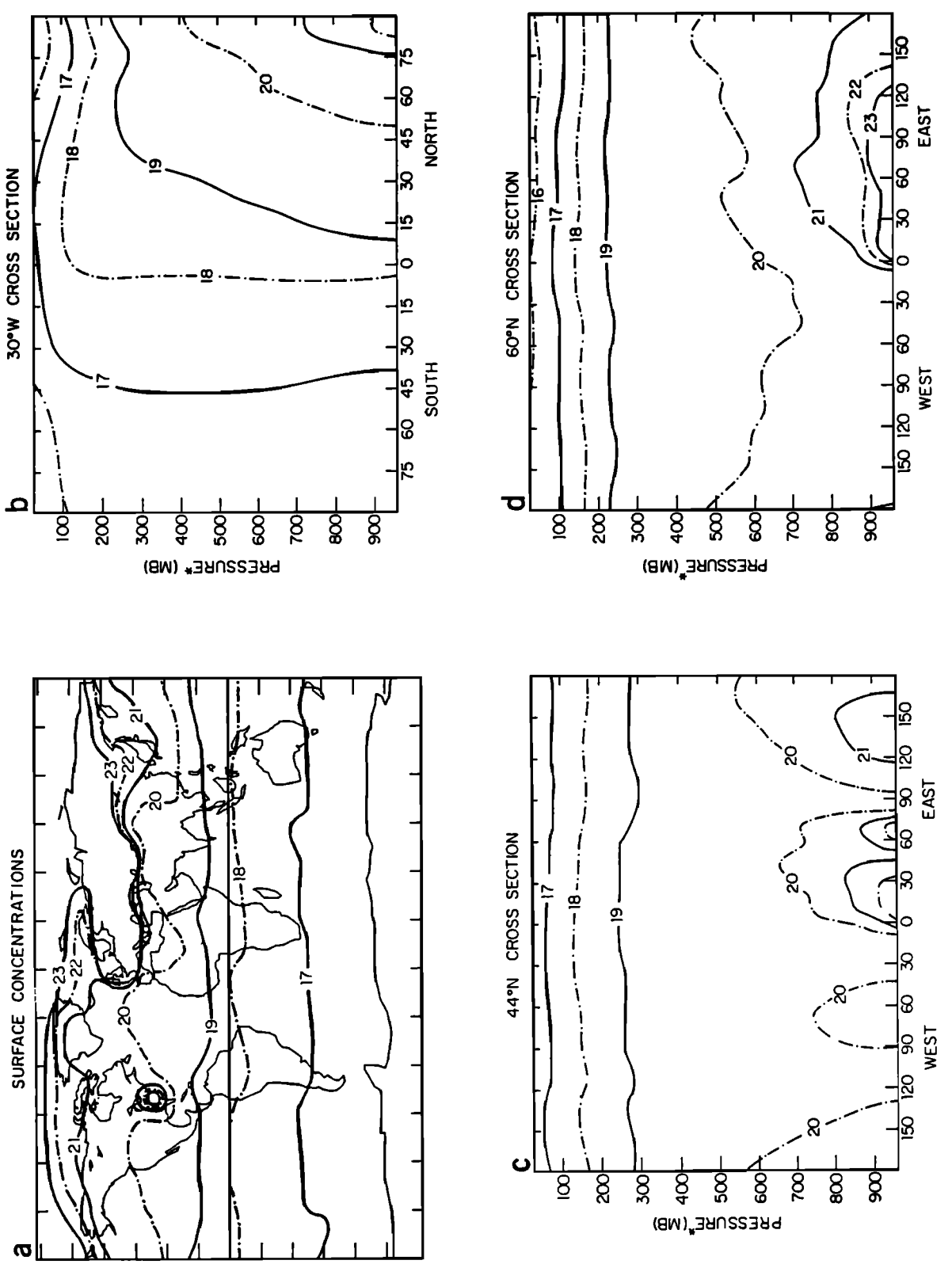

Fig. 5. Simulated global distribution of ^{85}Kr (in pCi/SCM) in January 1983. (*a*) Map of surface concentrations, (*b*) concentrations at 30°W, (*c*) concentrations at 44°N, (*d*) concentrations at 60°N. The ordinate "pressure*" is the σ vertical coordinate scaled to a global mean surface pressure of 984 mbar.

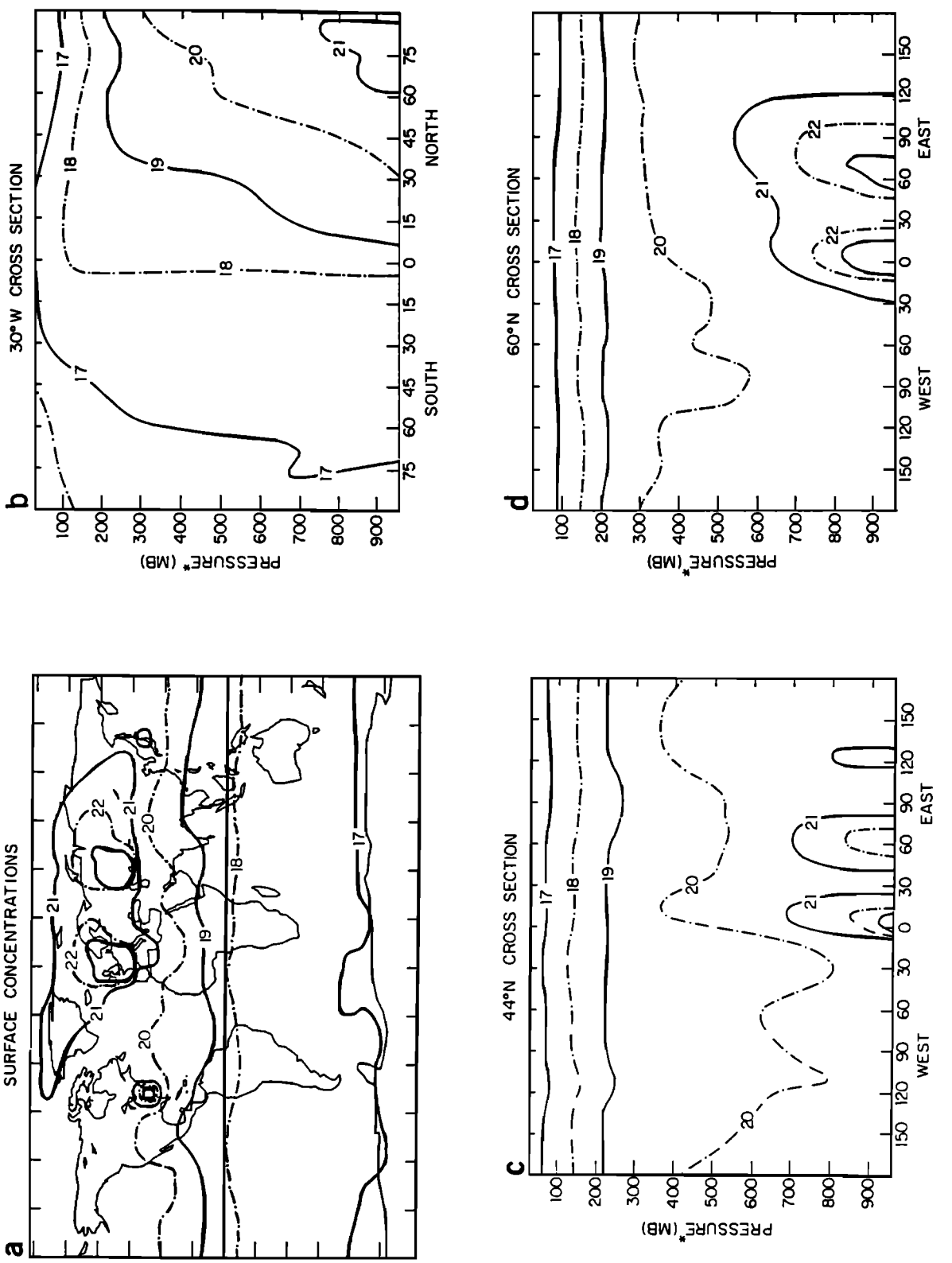

Fig. 6. Same as Figure 5, except in April 1983.

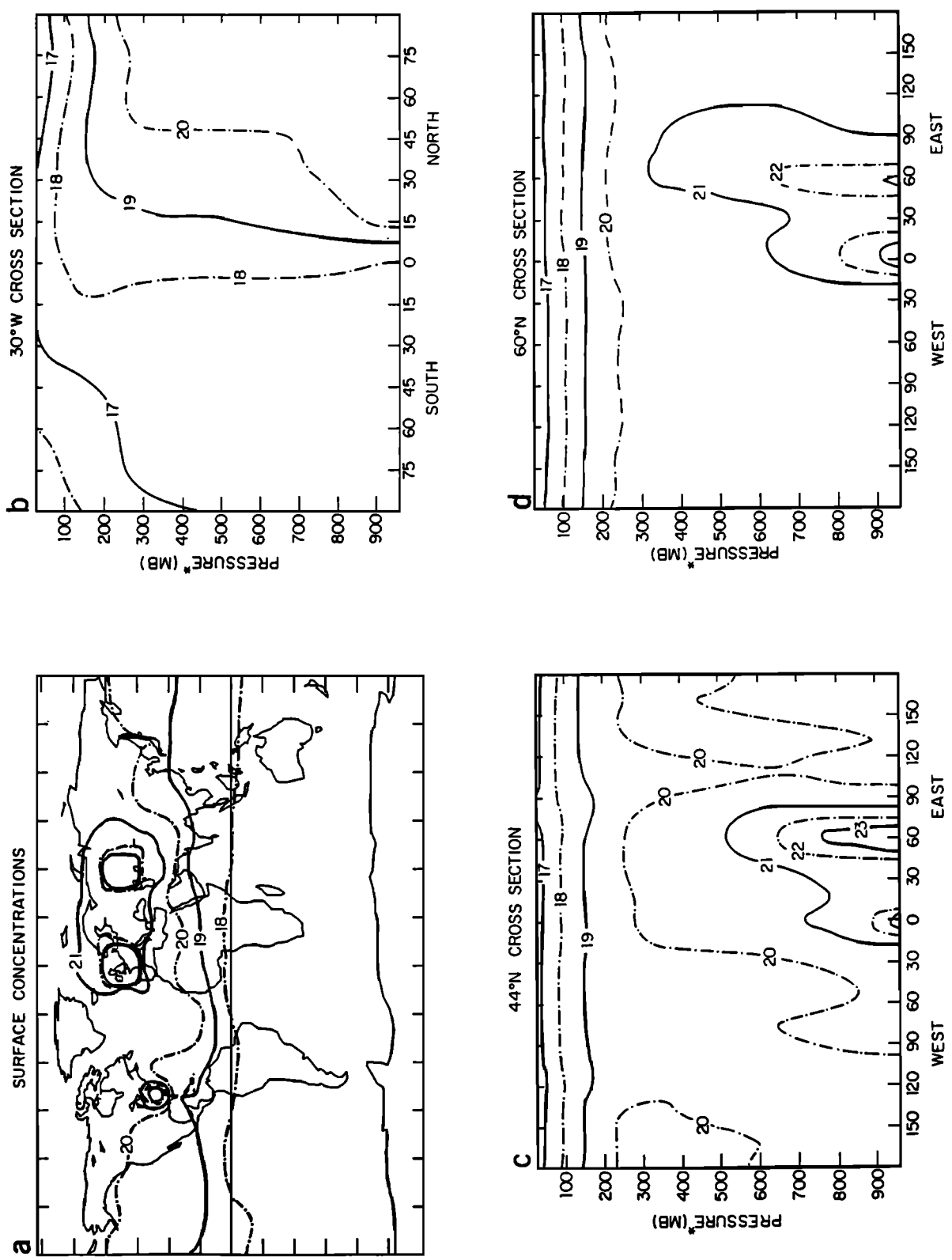

Fig. 7. Same as Figure 5, except in July 1983.

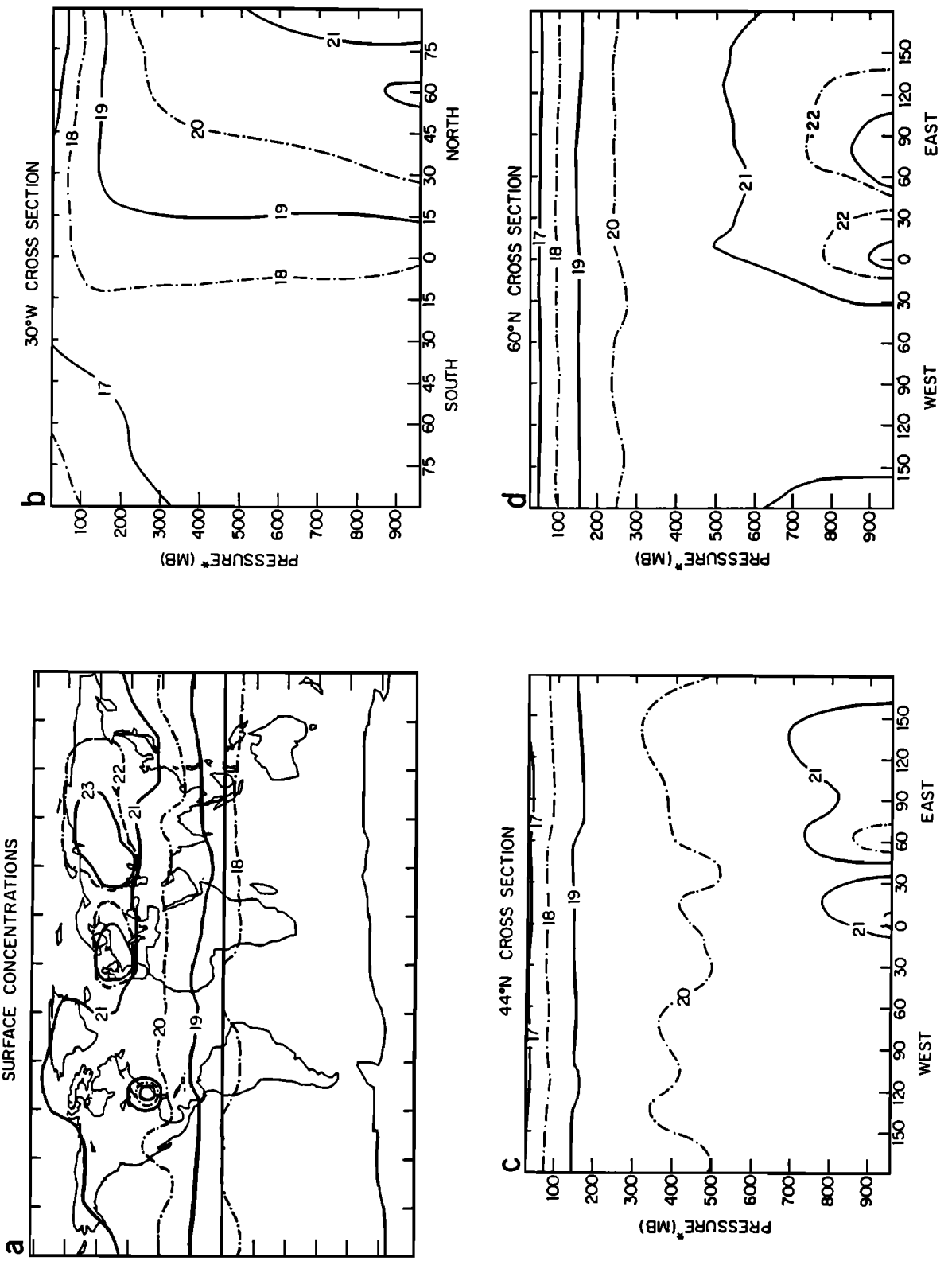

Fig. 8. Same as Figure 5, except in October 1983.

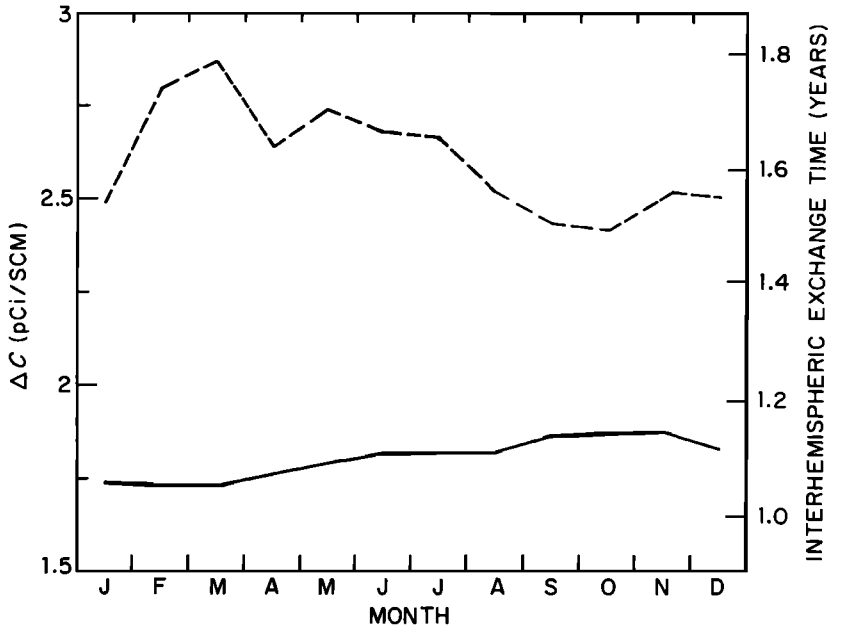

Fig. 9. Interhemispheric differences in ^{85}Kr concentrations predicted by the model for 1983, as a function of time of year: ΔC (solid line) and ΔA (dashed line). The value ΔC is the difference in global hemispheric mean concentrations, and ΔA is the difference in hemispheric mean surface concentrations at 30°W (middle of the Atlantic). The interhemispheric exchange time is the steady state value calculated from equation (7).

On the basis of the annual mean values of ΔC predicted by the CTM, we obtain $\tau_{ex} = 1.1$ years for each of the model years, in agreement with the result obtained from (5). As expected, the assumption of a steady state interhemispheric difference provides a satisfactory description for interhemispheric transport of ^{85}Kr in the CTM.

Weiss et al. [1983] used a similar steady state assumption to derive τ_{ex} from their latitudinal profiles. In this calculation, however, they used the interhemispheric differences derived from surface concentrations over the Atlantic (ΔA), instead of global hemispheric means (ΔC). Since concentrations over the Atlantic decrease with altitude in the northern hemisphere, ΔA is systematically larger than ΔC. Figure 9 shows the seasonal trends in ΔA and ΔC, as simulated by the model for 1983, and the corresponding values for τ_{ex} computed from (7). The annual mean value of τ_{ex} calculated from surface data is 1.6 years, almost 50% higher than the value determined from the three-dimensional analysis. We note also a large seasonality for ΔA, which is not present for ΔC; thus surface data give a misleading picture of seasonal variations in the interhemispheric exchange rate. From the lack of seasonality in ΔC, we see that the seasonal cycle in ΔA does not actually reflect seasonal differences in the rate of interhemispheric exchange; instead, it reflects seasonal changes in patterns of low-level advection from source regions.

Meridional transport across the equator in the CTM is accomplished by large-scale eddies which are resolved on a 8° × 10° grid and by diffusion associated with mesoscale mixing of air in deep convective storms of the intertropical convergence zone. The relative contributions of these mechanisms in the atmosphere is uncertain. In the CTM, convective diffusion provides 67% of the mean yearly cross-equatorial flux; the remainder is contributed by resolved advective processes. The parameterization adopted in the CTM to account for mesoscale mixing has the merit of providing an excellent simulation of interhemispheric transport for both ^{85}Kr and CFCs [*Prather et al.*, 1987], with the choice of a single parameter for subgrid diffusion (the horizontal length scale D of deep convection in the model). The large-scale latitudinal gradients observed at the surface provide, however, only one test of the model distribution. More research and observations, in the tropics in particular, are needed to establish the precise mechanisms for interhemispheric mixing.

4. Conclusions

Our research group has developed a three-dimensional model for long-range transport of pollutants in the troposphere, which is based on the winds and convection statistics from a general circulation model. We report excellent agreement between model simulations of the ^{85}Kr global distribution and six detailed latitudinal profiles observed over the Atlantic. In a previous study [*Prather et al.*, this issue], we found that the model reproduces correctly the observed time histories of chlorofluorocarbon concentrations at four different sites, two in each hemisphere. On the basis of these results we conclude that the model provides an adequate simulation of transport of long-lived tracers in the troposphere.

This three-dimensional model is a powerful tool to be used in conjunction with surface measurements. The measurements can be used to calibrate the model predictions; in turn, the model simulations allow limited surface measurements to be placed in a global context. In this manner, we determined global inventories of ^{85}Kr by scaling data from Atlantic cruises to the global distributions predicted by the model. The magnitude and the trend of the Soviet source were then calculated by subtracting the well-defined non-Soviet sources from the global inventories. We found that the Soviet source decreased by 25% between 1980 and 1983, which suggests that the Soviet Union may have cut back its production of plutonium during that period.

Because ^{85}Kr is a tracer of air from northern mid-latitudes,

study of its global distribution provides valuable insight on the long-range transport of anthropogenic pollutants. The model predicts that pollutants emanating from western Europe accumulate over the Arctic in winter and are transported southward in summer. Enhanced levels are expected over source regions in winter because of reduced convective activity. Transport from northern mid-latitudes to the southern hemisphere proceeds on a time scale of 1.1 years.

Acknowledgments. We are indebted to Frank Von Hippel (Center for Energy and Environmental Studies, Princeton University) for providing a copy of his report prior to publication. We would like to acknowledge helpful discussions with Frank Von Hippel and with Clarisa Spivakovsky and Jennifer Logan (Center for Earth and Planetary Physics, Harvard University). This reserach was supported by funds from the National Science Foundation (grant ATM-84-13153) and from the National Aeronautics and Space Administration (grant NAG5-719).

REFERENCES

Barrie, L. A., and R. M. Hoff, Five years of air chemistry observations in the Canadian Arctic, *Atmos. Environ.*, *19*, 1995–2010, 1985.

Grossman, R. F., and R. W. Holloway, Concentrations of krypton-85 near the Nevada Test Site, *Environ. Sci. Technol.*, *19*, 1128–1131, 1985.

Hansen, J., G. Russell, D. Rind, P. Stone, A. Lacis, S. Lebedeff, R. Ruedy, and L. Travis, Efficient three-dimensional global models for climate studies: Models I and II, *Mon. Weather Rev.*, *111*, 609–662, 1983.

Heidt, L. E., J. P. Krasnec, R. A. Lueb, W. H. Pollock, B. E. Henry, and P. J. Crutzen, Latitudinal distributions of CO and CH_4 over the Pacific, *J. Geophys. Res.*, *85*, 7329–7336, 1980.

Houze, R. A., Jr., and P. V. Hobbs, Organization and structure of precipitating cloud systems, *Adv. Geophys*, *24*, 225–315, 1982.

Karol', I. L., V. V. Babanova, and L. A. Romanovskaya, Global dispersion of "inert" gases in the atmosphere from ground sources, *Izv. Acad. Sci. USSR Atmos. Ocean. Phys.*, *12*, 787–794, 1976.

Khalil, M. A. K., and R. A. Rasmussen, Sources, sinks, and seasonal cycles of atmospheric methane, *J. Geophys. Res.*, *88*, 5131–5144, 1983.

Lowenthal, D. H., and K. A. Rahn, Regional sources of pollution aerosol at Barrow, Alaska, during winter 1979–80 as deduced from elemental tracers, *Atmos. Environ.*, *19*, 2011–2024, 1985.

National Council on Radiation Protection and Measurements, Krypton-85 in the atmosphere—Accumulation, biological significance, and control technology, *NCRP Rep. 44*, 1975.

Pannetier, R., Original use of the radioactive tracer gas krypton 85 to study the meridian atmospheric flow, *J. Geophys. Res.*, *75*, 2985–2989, 1970.

Phillips, N. A., A coordinate surface having some special advantage for numerical forecasting, *J. Meteorol.*, *14*, 184–185, 1957.

Prather, M. J., M. B. McElroy, S. C. Wofsy, G. L. Russell, and D. Rind, Chemistry of the global troposphere: Fluorocarbons as tracers of air motion, *J. Geophys. Res.*, this issue.

Rahn, K. A., Progress in arctic air chemistry, 1980–1984, *Atmos. Environ.*, *19*, 1987–1994, 1985.

Rahn, K. A., and R. J. McCaffrey, On the origin and transport of the winter Arctic aerosol, *Ann. N.Y. Acad. Sci.*, *338*, 486–503, 1980.

Russell, G. L., and J. A. Lerner, A new finite differencing scheme for the tracer transport equation, *J. Appl. Meteorol.*, *20*, 1483–1498, 1981.

Schroder, K. J. P., and W. Roether, The releases of krypton-85 and tritium to the environment and tritium to krypton-85 ratios as source indicators, in *Isotope Ratios as Pollutant Source and Behavior Indicators*, pp. 231–253, International Atomic Energy Agency, Vienna, Austria, 1975.

Steele, L. P., P. J. Fraser, R. A. Rasmusen, M. A. K. Khalil, T. J. Conway, A. J. Crawford, R. H. Gammon, K. A. Masarie, and K. W. Thoning, The global distribution of methane in the troposphere, *J. Atmos. Chem.*, in press, 1987.

Telegadas, K., and G. J. Ferber, Global atmospheric distribution of krypton-85 to 20 kilometers in 1973, *Health Saf. Lab. Environ. Q. U.S. Energy Res. Dev. Adm.*, *294*, 1975.

Von Hippel, F., D. H. Albright, and B. G. Levi, Stopping the production of fissile materials for weapons, *Sci. Am.*, *253*, 40–47, 1985.

Von Hippel, F., D. H. Albright, and B. G. Levi, Quantities of fissile materials in U.S. and soviet nuclear weapons arsenals, *Rep. PU/CEES 168*, Cent. for Energy and Environ. Stud., Princeton Univ., Princeton, N. J., 1986.

Weiss, W., A. Sittkus, H. Stockburger, and H. Sartorius, Large-scale atmospheric mixing derived from meridional profiles of krypton 85, *J. Geophys. Res.*, *88*, 8574–8578, 1983.

D. J. Jacob, M. B. McElroy, and S. C. Wofsy, Center for Earth and Planetary Physics, Harvard University, 29 Oxford Street, Cambridge, MA 02138.

M. J. Prather, NASA Goddard Institute for Space Studies, 2880 Broadway, New York, NY 10025.

(Received December 7, 1986;
revised April 8, 1987;
accepted April 9, 1987.)